Catalysis Today 158 (2010) 2–11

Contents lists available at ScienceDirect

Catalysis Today

journal homepage: www.elsevier.com/locate/cattod

Electrocatalytic activity of polypyrrole films incorporating palladium particles

Ana Mourato[a], Joana F. Cabrita[a], Ana M. Ferraria[b], Ana M. Botelho do Rego[b], Luisa M. Abrantes[a,*]

[a] CQB, Departamento de Química e Bioquímica, Faculdade de Ciências da Universidade de Lisboa, Campo Grande, 1749-016 Lisboa, Portugal
[b] Centro de Química-Física Molecular (CQFM) and Institute of Nanoscience and Nanotechnology (IN), Complexo Interdisciplinar, Instituto Superior Técnico, Technical University of Lisbon, Av. Rovisco Pais, 1049-001 Lisboa, Portugal

ARTICLE INFO

Article history:
Available online 1 August 2010

Keywords:
Polypyrrole
Palladium nanoparticles
Electroless precipitation
Electrocatalytic activity
Hydrazine
Modified electrodes

ABSTRACT

This work exploits the electroless precipitation approach for the incorporation of palladium in polypyrrole (PPy). Electrochemical and morphological analysis of PPy films prepared on Pt, under potentiostatic and potentiodynamic control, reveal the influence of the electrosynthesis conditions on the bulk and surface properties of the polymer. It is shown that, besides the pH of the $PdCl_2$ containing solutions, those PPy characteristics play an important role on the rate of the Pd uptake process. The resulting Pd(0)/Pdox ratio, size and surface distribution of the metallic particles on the film surface are analysed in detail and correlated to the electrocatalytic activity disclosed by the modified PPy electrodes towards the oxidation of hydrazine in KCl solution. In comparison to palladium thin coatings, a superior behaviour is achieved for PPy rough surfaces able to create uniform dispersions of sub-micron Pd particles, but the employment of polymer films with less coarse surfaces and/or an increasing in the amount and size of the Pd particles is disadvantageous for catalytic purposes.

1. Introduction

The use of electronically conducting polymers (ECPs) as supporting matrices for the immobilization of noble metal particles for electrocatalytic purposes (e.g. Pt, Pd, Au and Ag) has been subject of an extensive research [1,2]. Due to the ECPs porous structure and high surface area, it is possible to control the size and specific surface area as well as the dispersion of the catalyst metallic centers, on the polymeric matrix [1]. Additionally, ECPs may provide an efficient route for the flow of electronic charges to and from the nano/micro metal particles [3]. The incorporation of metal noble particles can be achieved by electroless precipitation [4–6], which takes place when the spontaneous polymer oxidation occurs with simultaneous reduction of the metal ions [5]. The only condition is that the metal ion reduction potential conforms to the potential range of the polymer conversion. This process is auto-sustained as far as the ECP is exposed to the metal containing solution, being only limited by the decreasing effective surface area of the polymer due to metal coverage [7]. Several studies have been reported using this methodology for the preparation of ECPs–Pd materials, e.g. Polyaniline–Pd [3,7–12] and Polypyrrole (PPy)–Pd [3,11–14].

The polymer properties, the nature and pH of the ion metal solution have been shown to influence Pd uptake process [3,14]. Kang et al. [11] have studied the effect of the redox state of PPy and the importance of the acidic medium concluding that when the reduced polymer is dipped in a solution containing Pd ions, an enhanced metal reduction rate occurs at the initial stage compared to the more oxidized state of the film; in this environment, the imine nitrogens of PPy were immediately protonated. Other factors, as the rate of Pd incorporation and the oxidation state in which those species are immobilized in the polymeric matrix, were also found to be dependent on the nature of the Pd containing solution. In fact, it has been reported [3,13] that using $Pd(NO_3)_2$ solutions, not only the rate of palladium uptake but also the Pd(0)/Pd(II) ratio are substantially higher than those obtained with $PdCl_2$ solutions; in the latter case, a predominance of Pd(II) species over Pd(0) is observed.

Hasik et al. [12], by means of X-ray photoelectron spectroscopy, examined the interactions between PPy (as powder) and Pd complexes present (general formula $PdCl_x(H_2O)_y$, $x+y=4$) in $PdCl_2$ solutions of different acidities. They concluded that the reduction of Pd(II) to Pd(0) with simultaneous oxidation of the polymer chain is favored in media where $[PdCl_2(H_2O)_2]$ is the predominant species.

The electrocatalytic activity of PPy films incorporating metal particles has been investigated for specific reactions such as the oxidation of methanol [15] and the oxidation of glucose and formic acid [16,17]. Dodouche and Epron [18] have also verified that PPy films as hosts for Pd particles were much more active and selective than the classical Al_2O_3–Pd catalyst for the reduction of nitrite ion in water; studies of Chen et al. [19] on the electrocatalytic hydrogenation of 4-chlorophenol, showed that this type of polymer supported catalysts provides higher performance and dechlorination efficiency than the bulk Pd. As described by Rao and Trivedi [20], composites prepared by the incorporation of pre-synthesised

* Corresponding author. Tel.: +351 21 7500890.
E-mail addresses: acmourato@fc.ul.pt (A. Mourato), luisa.abrantes@fc.ul.pt (L.M. Abrantes).

0920-5861/$ – see front matter © 2010 Elsevier B.V. All rights reserved.
doi:10.1016/j.cattod.2010.07.004

Pd nanoparticles during the growth of PPy films, display an homogeneous metallic dispersion and are more effective electrocatalytic materials for the oxidation of hydrazine than pristine PPy films.

Aiming to obtain ECP-based modified electrodes exhibiting interesting electrocatalytic properties, the present work focuses on the preparation of PPy–Pd films using the electroless precipitation approach for the incorporation of the metal particles in the polymeric matrix. Essential aspects for observing a suitable distribution, amount and size of the Pd particles deposited on the polymer matrix, are addressed. The polymer characteristics, e.g. electroactivity, thickness, porosity and morphology, imparted by the electrosynthesis conditions, as revealed by the electrochemical (cyclic voltammetry (CV), electrochemical quartz crystal microbalance (EQCM)) and scanning electron microscopy (SEM) characterization of PPy films prepared on Pt, under potentiostatic and potentiodynamic control; the rate and efficiency of the Pd uptake process, and its dependence on the pH of the $PdCl_2$ containing media, retrieved from the open circuit potential measurements and EQCM data. For palladium identification and particularly for its oxidation state assessment, the loaded polymers were also studied by X-ray photoelectron spectroscopy (XPS).

The strong influence of the mentioned aspects on the performance of the modified electrodes is clearly evidenced by the responses of the PPy–Pd films towards the anodic oxidation of hydrazine in KCl solutions. Although important catalytic anodic currents are recorded for most of the samples, in contrast to the featureless response of pristine PPy, the best behaviour is attained with polymer matrices bearing uniform dispersions of sub-micron Pd particles. Moreover, these modified electrodes display an electrocatalytic activity superior to bulk palladium.

2. Experimental

The monomer pyrrole (Py – Sigma–Aldrich, 99.99%) was purified by distillation under reduced pressure. The lithium perchlorate ($LiClO_4$ – Fluka, purity ≥ 99%) was recrystallized with ethanol. All aqueous solutions were prepared with Millipore-Q water (nominal resistivity of 18 MΩ at 25 °C).

PPy films were grown from 0.05 mol dm^{-3} pyrrole in 0.1 mol dm^{-3} $LiClO_4$ aqueous solutions, under potentiostatic and potentiodynamic control, on polycrystalline Pt electrode (A = 0.196 cm^2). Before each experiment, a mirror-finishing Pt surface was generated by hand-polishing the electrode in an aqueous suspension of successively finer grades of alumina (down to 0.05 μm). A saturated calomel electrode (SCE) and a Pt foil (2 cm^2) were used as reference and counter electrode, respectively, in a conventional three-compartment glass cell, with a glass frit separating the working and the counter electrodes compartments. Prior to the experiments, the solutions were deoxygenated with N_2 for 15 min. The potentiostatic growth of PPy was carried out at E = 0.65 V, (E_g) employing 60 and 120 s deposition times, t_g, being the polymer films designated thereafter as $PPy_{60\,s}$ and $PPy_{120\,s}$, respectively; the potentiodynamic synthesis of PPy was attained by cycling the potential between −0.80 and +0.80 V, for 6 cycles at a sweep rate (ν) of 100 mV s^{-1} ($PPy_{6c\_100\,mV/s}$) and for 4 cycles at ν = 50 mV s^{-1} ($PPy_{4c\_50\,mV/s}$).

The films were washed with Millipore-Q water and electrochemically characterized in 0.1 mol dm^{-3} $LiClO_4$ aqueous solution; before cycling the potential between −0.80 and +0.40 V at ν = 50 mV s^{-1}, the polymers were completely discharged by keeping the electrode at the initial potential for 10 min. A CHI Electrochemical Analyzer – 620A Model controlled by a computer was used in the electrochemical experiments.

For the electroless precipitation of palladium, the PPy films were reduced (−0.80 V for 10 min in 0.1 mol dm^{-3} $LiClO_4$ aqueous solution) and washed in Millipore-Q water and then immersed for different periods of time, 5, 10 min and overnight, in a $PdCl_2$ solution containing 100 ppm Pd(II) in either 0.125 mol dm^{-3} HCl (pH = 1) or in KCl saturated solution (pH = 6); the modified electrodes are nominated as $PPy_{60\,s}Pd_{x\,min}$, $PPy_{120\,s}Pd_{x\,min}$, $PPy_{4c\_50\,mV/s}Pd_{x\,min}$ and $PPy_{6c\_100\,mV/s}Pd_{x\,min}$.

The gravimetric measurements were performed in a 420 Model CH Instruments Electrochemical Quartz Crystal Microbalance. One compartment Teflon EQCM cell was used. The working electrode was a Pt coated (1000 å) 8 MHz AT-cut quartz crystal electrode (A = 0.20 cm^2), a Pt wire was employed as counter electrode, and the SCE as reference electrode.

Solutions containing 6 mM of hydrazine hydrochloride (HZ, analytical grade) in 0.5 M KCl (pH = 6) were prepared to evaluate the electrocatalytic activity of pristine PPy and PPy/Pd films. HZ oxidation was assessed by cycling the potential from 0.00 V to +0.60 V, at a scan rate of 50 mV/s.

Scanning electron microscopy was performed with a FEG-SEM JEOL 7001F system at an accelerating voltage of 15 keV for the assessment of the pristine and modified PPy films morphology. The modified electrodes were also examined with a Nanoscope IIIa Multimode Atomic Force Microscope (Digital Instruments, Veeco) at room temperature. The ex situ AFM images were obtained in tapping mode, using etched silicon tips (resonance frequency of ca. 300 kHz).

XPS measurements were performed with an XSAM800 (KRATOS) dual-anode spectrometer operated in the fixed analyzer transmission mode, with pass energy of 20 eV. XPS spectra were recorded with the non monochromatized AlKα radiation ($h\nu$ = 1486.6 eV, power = 10 mA × 12 kV). The samples were analysed in an ultra-high-vacuum chamber (∼10^{-7} Pa) at room temperature, using Take-Off Angles (TOA) of 90° and 30°. A lower TOA probes a shallower region of the surface than a larger TOA [21]. Spectra were recorded by a Sun SPARC Station 4 with Vision software (KRATOS) using a step of 0.1 eV both for specific regions and for the survey spectra. A Shirley background was subtracted, and curve fitting was carried out using Gaussian–Lorentzian products. X-ray source satellites were subtracted. No charge compensation (flood gun) was used. The binding energies were corrected using as a reference the binding energy of sp^3 carbon centred at 285 eV. For quantification purposes, the sensitivity factors were 0.25 for C 1s, 0.42 for N 1s, and 4.6 for Pd 3d.

3. Results and discussion

3.1. Electrochemical preparation and characterization of polypyrrole films

As other ECP, PPy can be electrochemically prepared from aqueous media, under potentiostatic control, namely at E_g = 0.65 V vs. SCE. The amount of deposited material, Δm, which can be estimated by EQCM [22], is obviously dependent on the selected deposition time t_g (or growth charge Q_g). However, as illustrated in the present case for films prepared using t_g = 60 s (Q_g = 30.7 mC cm^{-2}; Δm = 8.1 ± 0.5 mg cm^{-2}) and t_g = 120 s (Q_g = 68.1 mC cm^{-2}; Δm = 17.4 ± 0.5 mg cm^{-2}), the PPy electroactivity–polymer ability to undergo oxidation–reduction conversion – revealed by the pair of current waves in the cyclic voltammograms collected in monomer free electrolyte, Fig. 1a, do not display the same relation as the growth charge (Table 1).

Polypyrrole films can also be prepared by repetitive potential cycling, between the monomer oxidation potential (0.65 V) and −0.80 V. Under this electrochemical mode of polymerization, it is possible to change the potential sweep rate and the number of cycles, originating films with distinct characteristics.

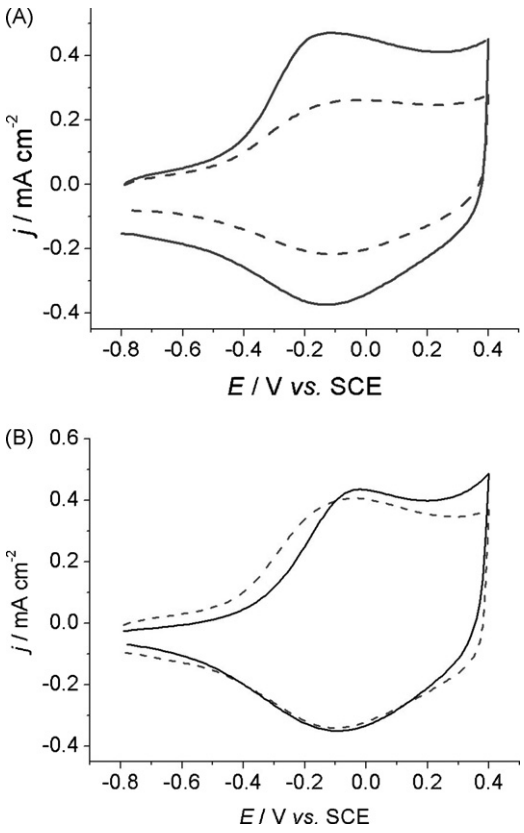

Fig. 1. Redox behaviour of PPy films (A) potentiostatically prepared at E_g = 0.65 V, using t_g = 60 s (broken line) and t_g = 120 s (full line) in 0.1 M $LiClO_4$ aqueous solution; υ = 50 mV/s and (B) deposited under potentiodynamic control using 6 potential cycles at υ = 100 mV/s (full line), 4 potential cycles at υ = 50 mV/s (broken line).

It is well known that ECP properties are determined by the electrochemical mode and conditions employed in the synthesis [23,24]. Although the polymer electroactivity has been often used as a simple basis of comparison [25,26], systematic studies allow to define different electrochemical parameters that led to films displaying similar electroactivities [8]. It is the case for polypyrrole, potentiodynamically prepared with 4 and 6 cycles at 50 and 100 mV/s ($PPy_{6c\_100\,mV/s}$, $PPy_{4c\_50\,mV/s}$) respectively, or at constant potential (E = 0.65 V) for 120 s ($PPy_{120\,s}$). Fig. 1b depicts the redox behaviour of these films; the charges involved in the conversion and the identical shape of the recorded voltammograms confirm their similar electroactivity. Thus, such preparative conditions have been selected to analyse other properties of the PPy layers including the ability to promote the electroless precipitation of Pd.

3.2. Electroless precipitation of palladium on PPy films

The electroless precipitation of metal particles on ECP is restricted to films with active nitrogen-containing surfaces. The most studied of this group is polyaniline (PAni). PAni presents different oxidation states running from the non-conducting leucoemeraldine which upon oxidation forms the protonated emeraldine (conducting) and further oxidation originates pernigraniline, a deprotonated form of PAni. The electroless precipitation of metal particles on PAni takes place when spontaneous deprotonation of emeraldine (to pernigraniline) occurs with simultaneous reduction of the metal ion which act as oxidizing species in solution [27]. Since in acidic media pernigraniline protonates spontaneously, the process is self-sustained until the surface is covered by the metal. Due to the potential domain where both reactions happen, the process is particularly suitable for noble metal reduction.

Table 1
Characteristic parameters of the redox conversion of PPy films potentiostatically grown using different deposition times (charges).

t_g/s	Q_g/mC cm^{-2}	E_p^{ox}/V	E_p^{red}/V	Q^{ox}/mC cm^{-2}	Q^{red}/mC cm^{-2}	Q^{ox}/Q^{red}
60	30.7	−0.10	−0.11	3.8	3.2	1.2
120	68.1	−0.17	−0.12	6.0	5.0	1.2

Table 2
Change on the oscillating quartz crystal frequency coated by PPy films prepared under different electrochemical modes and respective increase in mass up to 50 s and 10 min immersion times in 0.125 M HCl + 100 ppm $PdCl_2$ solution (pH = 1) and in 100 ppm $PdCl_2$ in saturated KCl (pH = 6).

PPy (solution pH)	Immersion time			
	50 s		600 s	
	Δf/Hz	Δm/μg cm^{-2}	Δf/Hz	Δm/μg cm^{-2}
$PPy_{120\,s}$ (pH = 1)	−176.08	1.20	−323.91	2.25
$PPy_{120\,s}$ (pH = 6)	−50.22	0.30	−153.57	1.06
PPy_{6c} (pH = 1)	−71.88	0.52	−320.41	2.23
PPy_{6c} (pH = 6)	−74.23	0.50	−96.93	0.67

PPy is also a polymer with active nitrogen-containing surface; it also presents a range of intrinsic oxidation states [28], from the fully reduced neutral PPy to the 25% doped salt which undergoes deprotonation under oxidation, thus giving rise to 25% de-protonated PPy. Thus PPy, as PAni, can promote Pd precipitation, through reduction of the metal ion in acid solution, to its elemental form.

Taking into account that the electroless precipitation of metal particles depends on the polymer surface exposed to the electrolyte, it is expected that the films morphology plays an important role in the process efficiency. In spite of the above mentioned analogy in electroactivities of PPy films prepared under different electrochemical conditions, namely $PPy_{6c\_100\,mV/s}$, $PPy_{4c\_50\,mV/s}$ and $PPy_{120\,s}$, the polymer layers display distinct morphologies as observed by SEM and AFM, Fig. 2 and Fig. 2B respectively. The films grown potentiodynamically are formed by larger nodules than the potentiostatically deposited one. The difference in organization and grain size is possibly a result of the fast and successive redox conversions during the deposition.

In what concerns the composition and pH of $PdCl_2$ aqueous solutions employed for Pd uptake, it has been claimed that low acidity and the replacement of protons by potassium cations may facilitate the reduction of Pd(II) to Pd(0) [12,14]. In an attempt to appraise the influence of both issues, hydrochloric acid and potassium chloride solutions (pH = 1 and 6, respectively) containing the same concentration of metal ion, have been used.

A first direct evaluation of the Pd electroless precipitation, accomplished by immersing the prior reduced (−0.80 V for 15 min) PPy modified electrodes in the Pd(II) containing solution, is the measurement of the open circuit potential evolution with time. In the data obtained for Pd uptake from pH = 1 solution, presented in Fig. 3, it is observed an initial rapid increase in the OCP followed by a plateau at about 0.35 V. The slight divergences in approaching the constant potential value could be correlated to different gradients for the diffusion of Pd(II) species in the bulk polymer, but it would be speculative. This qualitative information needs a better appraisal as the one given by EQCM.

Changes in the oscillating PPy coated quartz crystal frequency during the palladium uptake for 10 min from both above mentioned solutions, of different pH but containing the same concentration of metal ion, recorded for $PPy_{120\,s}$ (the film showing a relatively regular and homogeneous surface) and for $PPy_{6c\_100\,mV/s}$ (rough surface) are displayed in Fig. 4. The respective increase in mass, Table 2, has been evaluated using the Saurbery equation [22]. The mass varia-

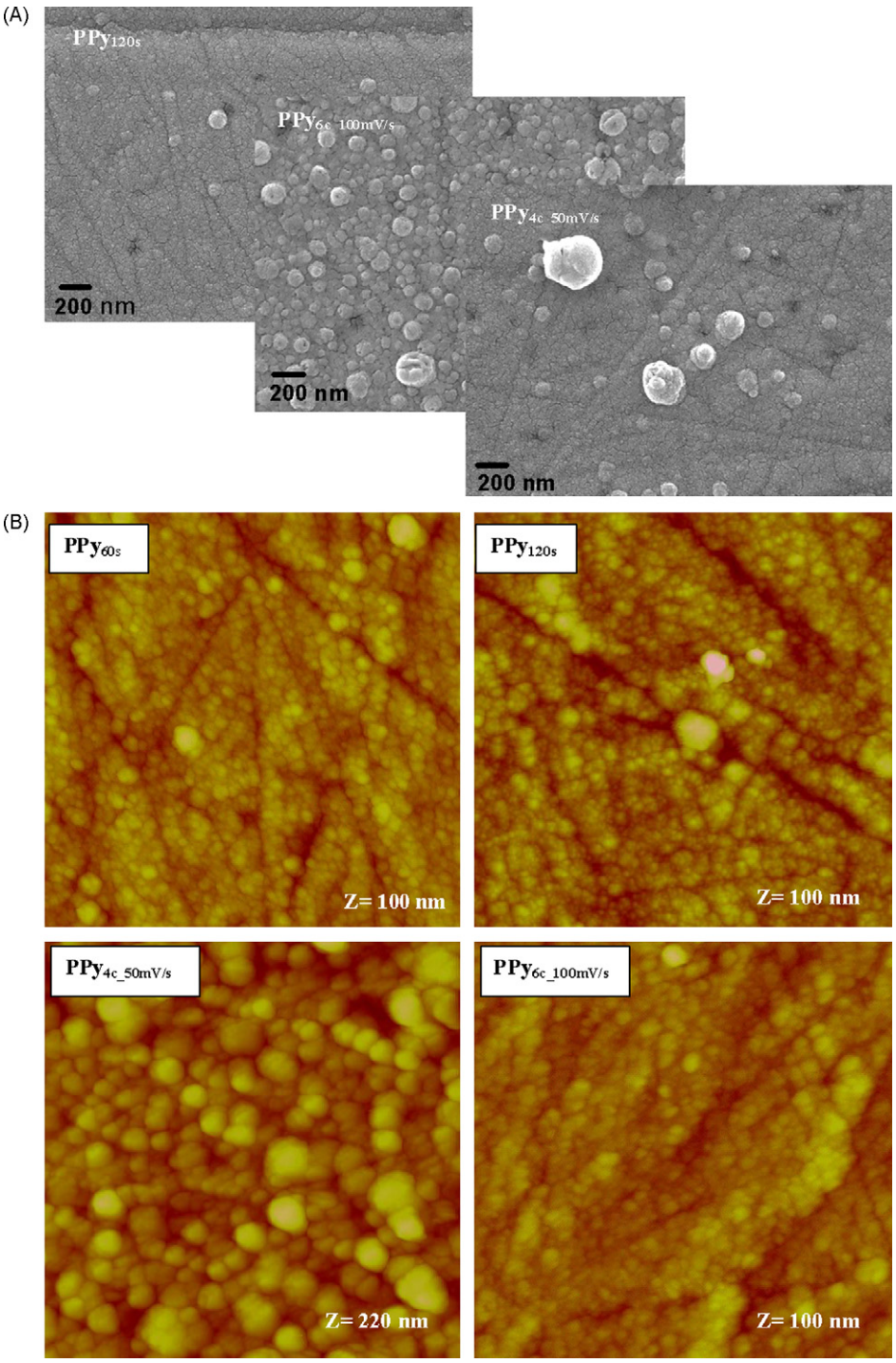

Fig. 2. SEM (A) and AFM (B) images of PPy films prepared under different electrochemical modes and conditions.

tion throughout the electroless precipitation, revealed that the total amount of palladium species, e.g. Pd(0) and/or Pd(II) ionic species that can act as dopants of the PPy films and be retained in the polymer matrix or reduced with it [12], is much higher at pH = 1, than if the deposition process is carried out at pH = 6.

For $PdCl_2$ solution at pH = 1, well noticed is the drastic augment in mass (decrease in frequency) that occurs for $PPy_{120\,s}$, during the first 50 s, reaching around one half of the total mass rise. In contrast, when a surface with higher roughness is used, $PPy_{6c\_100\,mV/s}$, there is no important initial increase in the rate of Pd uptake process which keeps fairly constant from 50 to 450 s, being thereafter the frequency (mass) variation negligible. At an initial stage, the incorporation of Pd(II) occurs simultaneously with the electroless precipitation of Pd(0) at the active sites of the PPy surface, as the EQCM data suggests. Due to the coarse nature of the surface of $PPy_{6c\_100\,mV/s}$ films, relatively more active sites are exposed to the solution and Pd(0) precipitation is expected to occur in a larger extent in comparison to $PPy_{120\,s}$, notwithstanding, as the surface coverage by Pd(0) increases, further diffusion of Pd species leading to the incorporation of Pd ions and/or precipitation of Pd(0) inside the film is hindered. Accordingly, in PPy prepared potentiodynamically (Fig. 4B), the ratio of Pd(0)/Pd(II) obtained with the pH = 6 solution is very likely higher than for palladium uptake at pH = 1, in agreement with the literature [12]. Due to the process

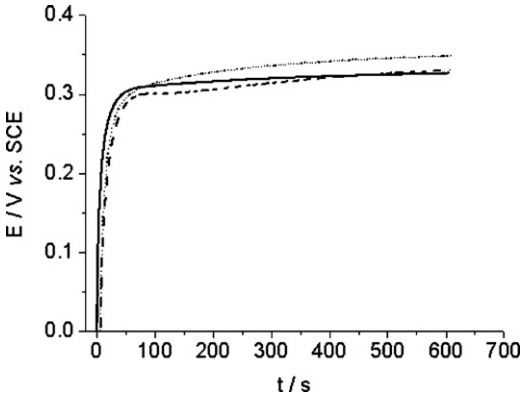

Fig. 3. Open circuit potential evolution with time for $PPy_{6c.100\,mV/s}$ (full line), $PPy_{4c.50\,mV/s}$ (broken line) and $PPy_{120\,s}$ (dotted line) immersed in 0.125 M HCl + 100 ppm $PdCl_2$ solution, pH = 1.

complexity and the large difference in the chloride ion content, the obtained EQCM results could not be used to discuss in depth the influence of the K^+ presence. However, contrasting Fig. 4A and B, it is clear that the polymer film morphology plays the primary role in the initial period, and a overturned effect of the solution pH may occur. As the largest amount of incorporated palladium species was obtained with the pH = 1 solution, such conditions were followed in the subsequent studies.

After Pd uptake for 10 min from pH = 1 solution, a similar increase in mass (2.2 $\mu g\,cm^{-2}$, Table 2), was obtained for both studied films. It represents the amount of Pd species in the polymer as a whole, being not possible from EQCM data to retrieve the relative contents in Pd(0) and Pd ionic species.

Aiming for further information, especially in what concerns the oxidation state, XPS analysis of the PPy films loaded with Pd at pH = 1 has been carried out. XPS regions Pd 3d, N 1s, C 1s, Cl 2p and O 1s were analysed. Carbon and oxygen can be present both in the system Pd–PPy and under the form of carbonaceous and oxide contamination. Moreover, O 1s is overlapping the region Pd 3p turning the qualitative and quantitative analysis quite hard. Being palladium and nitrogen the only elements which do not exist in any possible contaminations, only two regions, Pd 3d and N 1s, will be fully discussed in the following. Fig. 5 shows the detailed XPS regions Pd 3d and N 1s for samples $PPy_{120\,s}Pd_{10\,min}$ and $Ppy_{6c.100\,mV/s}Pd_{10\,min}$, taken at a TOA = 30°. Qualitatively, they are very similar between each other and to all the other samples as well as to other analysis angles.

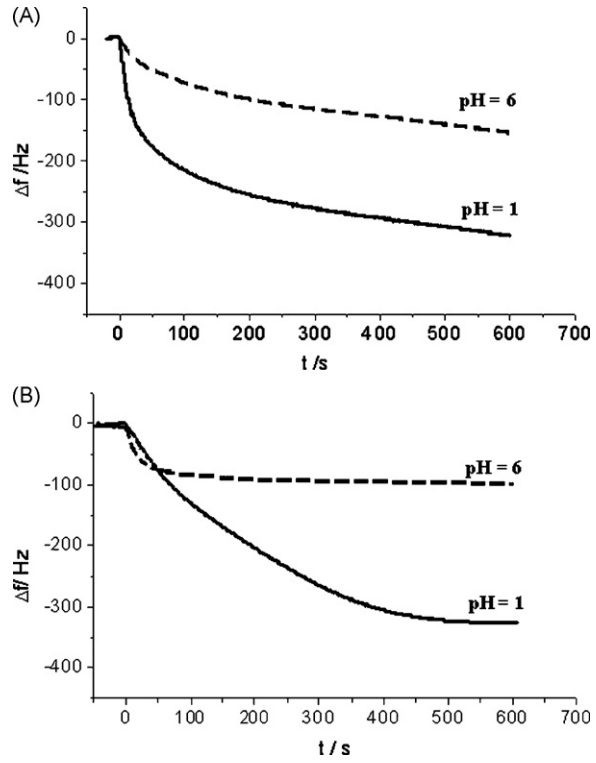

Fig. 4. Resonant frequency change in the oscillating quartz crystal coated by $PPy_{120\,s}$ (A) and $PPy_{6c.100\,mV/s}$ (B) during the electroless precipitation of palladium from 0.125 M HCl + 100 ppm $PdCl_2$ solution, pH = 1 (full line) and 100 ppm $PdCl_2$ in saturated KCl, pH = 6 (broken line).

Pd 3d was fitted with three doublets with doublet separations of 5.2 ± 0.2 eV. The region is dominated by an intense peak (Pd $3d_{5/2}$) centred at 335.3 ± 0.2 eV assigned to Pd(0). The computed Auger parameter Pd $3d_{5/2}$, $M_5N_{45}N_{45}$ = 663.1 (±0.4) confirms this assignment.

The second peak (Pd $3d_{5/2}$) is centred at 336.8 ± 0.2 eV which is assigned, in the literature, to Pd(II) bound to oxygen [3]. Finally, the Pd $3d_{5/2}$ component for the third one is centered at 338.3 ± 0.2 eV and could be attributed to Pd(IV) or to Pd(II), coordinated or not to N atoms, but always having in its neighbourhood chlorine atoms [12,29]. Nevertheless, the first hypothesis should be disregarded, since in the system under study it is not expectable to have palladium under the form of Pd(IV). This Pd(II) (identified in Fig. 5 as

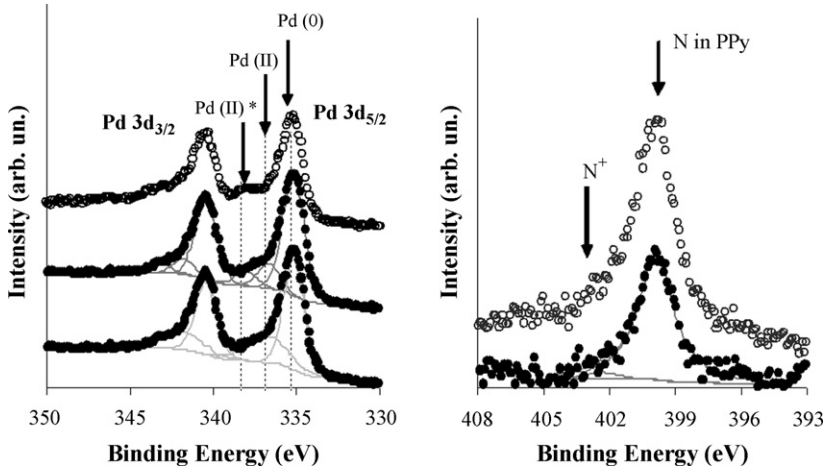

Fig. 5. XPS regions (A) Pd 3d and (B) N 1s at TOA = 30° of $PPy_{120\,s}Pd_{10\,min}$ (full symbols) and $PPy_{6c.100\,mV/s}Pd_{10\,min}$ (open symbols). For distinction between Pd(II) and Pd(II)* see text.

Table 3
XPS quantitative analysis.

Atomic ratio	TOA (°)	$PPy_{120\,s}Pd_{x\,min}$		$PPy_{6c\_100\,mV/s}Pd_{x\,min}$	
		$x=5$	$x=10$	$x=5$	$x=10$
Pd^0/Pd_{ox}	90	3.3	2.7	2.7	2.1
	30	3.5	3.1	3.2	2.4
Pd/N (±10%)	90	1.2	0.9	0.7	0.4
	30	1.9	1.0	1.2	0.5
C/N (±10%)	90	8.8	10.5	7.1	6.2
	30	12.4	14.9	9.7	7.8

Pd(II)*) coming from the compound $PdCl_2$, should exhibit a stoichiometric ratio Pd/Cl = 1:2. This is exactly the value obtained for the XPS ratio Pd(II)*/Cl in all the modified electrodes confirming the soundness of the assignment. Peaks at higher binding energies correspond to the second (and weaker) components of each doublet (Pd $3d_{3/2}$).

In N 1s the main peak centred at 399.9 ± 0.2 eV is typical of nitrogen in the polypyrrole chain [30]. Around 402.5 eV a much less intense peak assignable to N^+ can be found [31]. Table 3 summarizes quantitative data for all the analysed samples where the electroless palladium precipitation was carried under pH = 1.

In all cases the existence of palladium at the surface (±10 nm in depth) is observed both in reduced and oxidized form. The ratio Pd^0/Pd_{ox} is obtained from the ratio between fitted components to the Pd $3d_{5/2}$ peak. This means that the associated error may be very large and differences observed should not be valued. Although the only serious comment on those ratios is that they all have the same order of magnitude, a slight tendency to decrease with time can be inferred; this decrease is compatible with a progressive deposition of Pd(II) species on the surface of the polymer without further reduction to Pd(0), as the active sites of the PPy surface for precipitation of Pd(0) become occupied.

The ratio Pd/N is also very interesting: QCM data reveal that the amount of palladium increases with time. However, for both sample types, a decrease of the XPS ratio Pd/N with time is observed. This result is compatible with the deposited palladium being much more spread over the entire surface at the t_d = 5 min and much more aggregated (even if the total number of Pd atoms increases) at t_d = 10 min [32]. Comparison of those same ratios at TOA = 90° and TOA = 30° also confirms the preceding assumption: they are almost invariant for cases where a strong aggregation (island structure) exists, and exhibit a large variation when an uniform film covers a smooth substrate [33]. The Pd/N ratio also allows the comparison of $PPy_{120\,s}Pd_{x\,min}$ and $PPy_{6c\_100\,mV/s}Pd_{x\,min}$ samples: for both 5 and 10 min Pd deposition times, Pd/N ratio is larger for $PPy_{120\,s}$ than for $PPy_{6c\_100\,mV/s}$. But, at least for t_d = 10 min, Table 2 shows that the amount of palladium incorporated is very similar for both samples.

To make data from both sources compatible, we should remember that roughness is much higher in $PPy_{6c\_100\,mV/s}$ film. This means that there is a larger specific surface available in $PPy_{6c\_100\,mV/s}$ for Pd embedment. However, for the fraction of particles inside the pores, the XPS Pd signal will be much more attenuated than in the case of those on the external surface. Therefore, for the same number of particles, Pd signal will be larger when they are on a smooth surface. Finally, stoichiometric C/N ratio is 4 in polypyrrole. XPS ratio is always larger than 4 and increases from TOA = 90° to TOA = 30° confirming that a significant carbon XPS signal comes from surface contamination.

Both PPy films modified by the Pd loading achieved after 5 and 10 min immersion times were examined by SEM. To avoid masking the presence of Pd, the images, depicted in Fig. 6, were obtained without any sample pre-treatment; even so it is possible to detect small Pd particles and their slight increase with the immersion time. Small clusters of about 20 nm diameter are observed for $PPy_{6c\_100\,mV/s}Pd_{10\,min}$.

Contrasting the AFM topographic images of PPy films before and after Pd incorporation, it is hard to recognize the presence of Pd. However by mapping the phase, it is possible to detect local changes and to distinguish the presence of Pd as evidenced in Fig. 7. The existence of Pd particles and clusters of different size can be correlated with the heterogeneous nature of the polymer film surface: very small particles well dispersed on the polymer surface are formed on potentiostatically prepared PPy (A and B), whereas larger particles and clusters can be seen when the polymer is deposited by potential cycling (C, D and E) and a much rougher surface is produced. In this case the formation of Pd(0) inside the layer and at the surface is likely; indeed images D and E suggest that the Pd particles also fill the PPy pores resulting in a quite homogeneous distribution

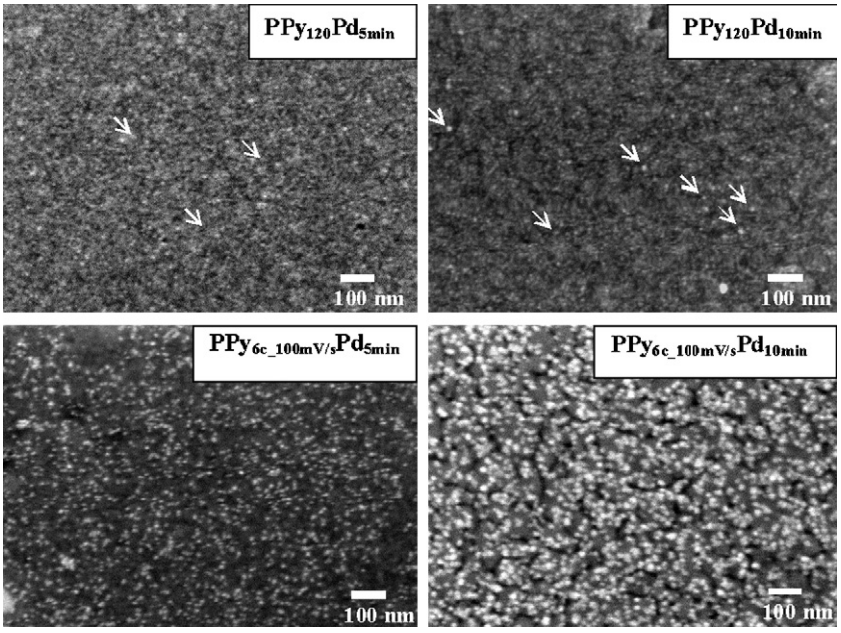

Fig. 6. SEM images of the Pd loaded PPy films.

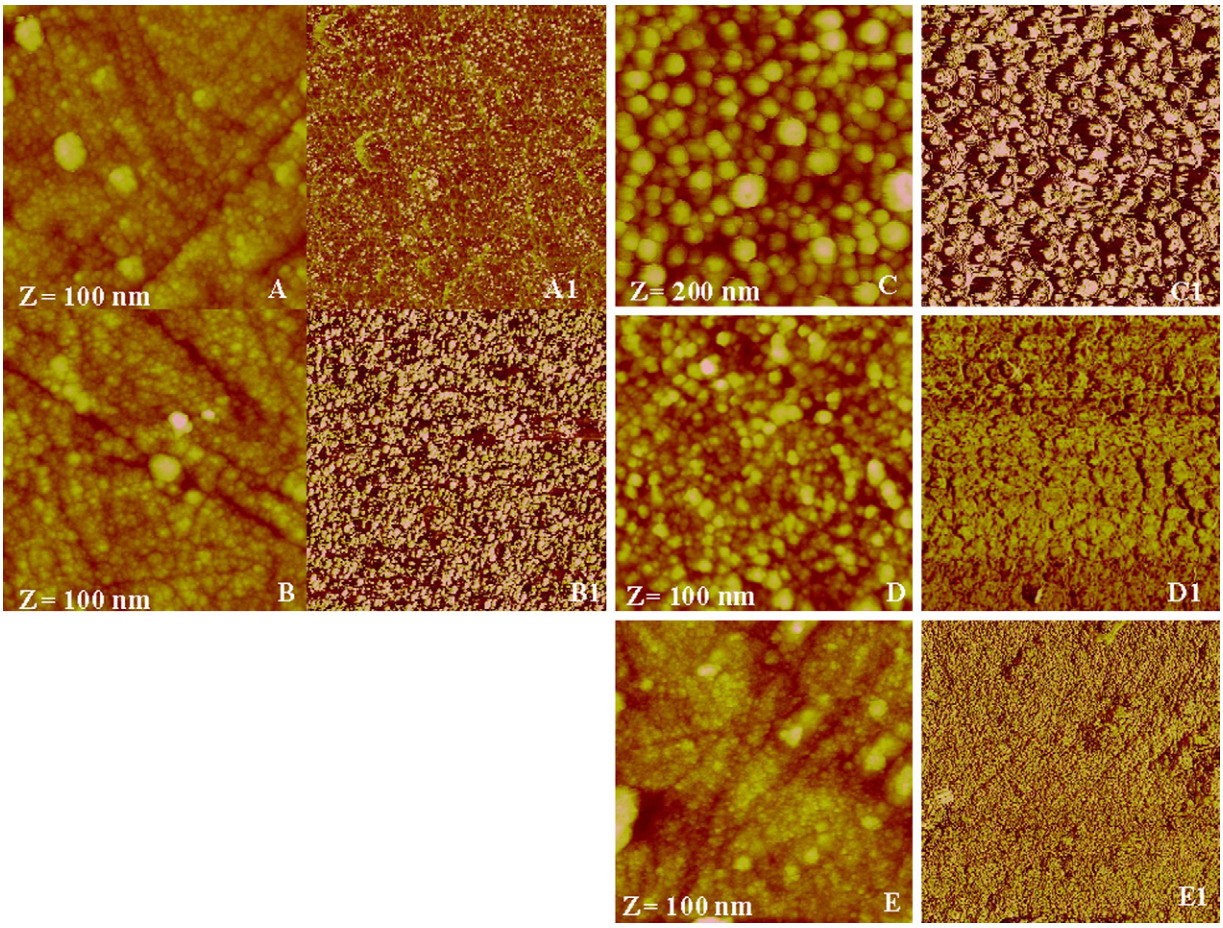

Fig. 7. Topographic images of the modified electrodes: $PPy_{60\,s}Pd_{10\,min}$ (A), $PPy_{120\,s}Pd_{10\,min}$ (B), $PPy_{4c\_50\,mV/s}Pd_{10\,min}$ (C), $PPy_{6c\_100\,mV/s}Pd_{5\,min}$ (D) and $PPy_{6c\_100\,mV/s}Pd_{10\,min}$ (E). The corresponding phase images recorded simultaneously with the topographic images are denoted by A1, B1, C1, D1 and E1, respectively ($Z = 100^{\circ}$); window size 2 μm × 2 μm.

and apparently a smoother surface morphology develops as the Pd uptake time increases.

These observations are in good agreement with the information provided by the above mentioned XPS analysis which pointed to the aggregation of Pd particles at $t_d = 10$ min.

The whole set of data collected for the characterization of the prepared PPy–Pd films suggests differences in the electrocatalytic behaviour of the modified electrodes, in spite of carrying the Pd uptake from identical solutions (in composition and concentration) and of using polymer layers with similar electroactivities.

3.3. *Electrocatalytic properties of PPy–Pd modified electrodes*

Hydrazine (HZ) is of relevance in chemical and pharmaceutical industries [34]. Intensive research has been developed focusing either its selective determination [35] or demanding its electrocatalytic oxidation [34,36].

The accepted mechanism for the irreversible oxidation of hydrazine, in 5–10 pH range, involves two steps [34], i.e., a single electron transfer (rate determining) followed by a 3-electron process to give N_2 as final product, according to Eqs. (1) and (2):

$$N_2H_4 + H_2O \rightarrow N_2H_3 + H_3O^+ + e^- \quad (1)$$

$$N_2H_3 + 3H_2O \rightarrow N_2 + 3H_3O^+ + 3e^- \quad (2)$$

One of the few reports on the response of PPy–Pd towards HZ oxidation considers a free standing film formed by a one-step synthesis procedure [20] and reveals a promising behaviour; although the HZ oxidation occurs at more positive potentials on the prepared membrane than on pure Pd, the developed current is much higher. The difference has been attributed to the lower size of the Pd particles in PPy–Pd compared to the polycrystalline nature of the pure Pd film. Thus, it was considered of interest to choose the oxidation of HZ, in neutral (pH = 6) media, to appraise the electrocatalytic activity of the PPy films modified by the electroless precipitation of Pd particles.

It is known that oxidation/dissolution of palladium may occur at relatively high potentials [37,38]. The voltammograms depicted in Fig. 8 show that, in KCl solution (pH = 6), substantial oxidation of the Pd embedded particles occurs when the potential is scanned to values higher than 0.40 V. Therefore, such potential region must be avoided in an analysis of the behaviour of the PPy–Pd films towards the oxidation of HZ, particularly when information on the reproducibility/stability of the modified electrodes is also envisaged.

The current responses collected for the differently prepared PPy and PPy–Pd films in the presence of HZ (6 mM) in KCl solution can be seen in Fig. 9. Comparison with the behaviour displayed by bulk palladium electrodes is also relevant; since the evaluation of the real surface area of Pd particles in each PPy–Pd modified electrodes, is out of the scope of the present work, completely Pd coated PPy films, prepared by prolonged (overnight) electroless precipitation of Pd in each case, have been used for that purpose and the current densities referred to the geometric electrode area.

At pristine PPy electrodes the voltammograms are featureless, revealing the inactivity of the base polymer layers towards the HZ oxidation. On the other hand, at Pd electrodes the peak current occurring at 0.28 V (coated PPy_{120}) and at 0.26 V (coated $PPy_{6c\_100\,mV/s}$) reveals the HZ oxidation. For PPy incorporating

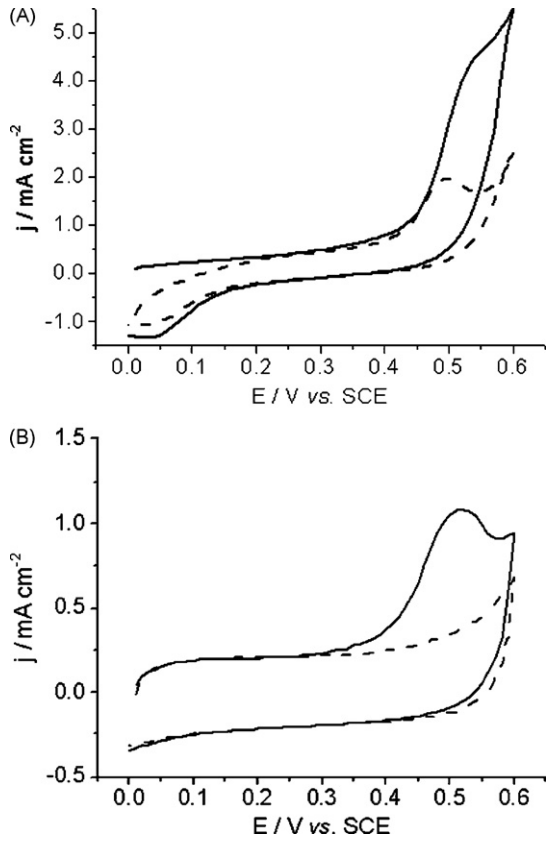

Fig. 8. Linear sweep voltammograms of the $PPy_{120\,s}Pd_{10\,min}$ (A) and $PPy_{6c.100\,mV/s}Pd_{5\,min}$ (B) modified electrodes in KCl solution (pH = 6); υ = 50 mV/s. 1st cycle (full line) and 2nd cycle (broken line).

Table 4
Voltammetric characteristics of PPy–Pd modified electrodes in KCl + 6 mM HZ solution (pH = 6).

	E_p^{ox}/V	j/mA cm^{-2}
$PPy_{60\,s}Pd_{10\,min}$	0.304	1.45
$PPy_{120\,s}Pd_{5\,min}$	0.270	3.84
$PPy_{120\,s}Pd_{10\,min}$	0.270	3.79
$PPy_{120\,s}Pd_{overnight}$	0.282	4.07
$PPy_{4c.50\,mV/s}Pd_{10\,min}$	0.326	1.66
$PPy_{6c.100\,mV/s}Pd_{5\,min}$	0.227	4.53
$PPy_{6c.100\,mV/s}Pd_{10\,min}$	0.325	1.86
$PPy_{6c.100\,mV/s}Pd_{overnight}$	0.260	4.05

the Pd particles, Table 4 summarizes the characteristics of the voltammograms shown in Fig. 9. In comparison with the data at Pd coated PPy electrode, an increase in the peak current and a decrease in the oxidation potential, where the oxidation of HZ takes place, is observed for $PPy_{6c.100\,mV/s}Pd_{5\,min}$ modified electrode (Fig. 9B). However, when the electroless Pd uptake is carried out for longer periods, namely, for $PPy_{6c.100\,mV/s}Pd_{10\,min}$, the oxidation rate decreases and a larger overpotential is required for HZ oxidation. This behaviour is to be expected, taking into account the earlier discussed characteristics of the modified electrodes. In fact, after 10 min Pd uptake, same metallic clusters are formed which are exposed to the electrolyte solution instead of submicron individual Pd particles. In the case of $PPy_{120\,s}$ embedding Pd particles after electroless precipitation for 5 or 10 min, Fig. 9D, and again in comparison with the Pd coated electrode, the peak current is slightly smaller but the peak potential shifts to less positive values (Table 4). This last feature attributable to the small size of incorporated Pd particles, also confers electrocatalytic activity towards the oxidation of HZ to this type of modified electrodes.

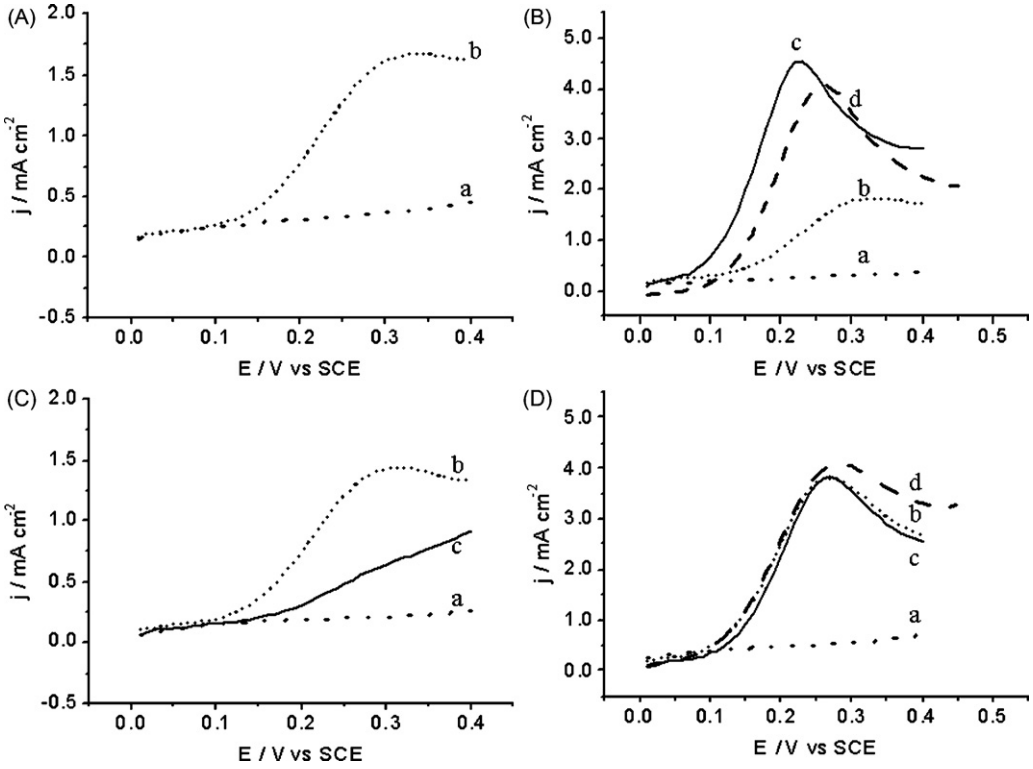

Fig. 9. Linear sweep voltammograms of the modified electrodes: (A) $PPy_{4c.50\,mV/s}$ (a) and $PPy_{4c.50\,mV/s}Pd_{t=10\,min}$ (b); (B) $PPy_{6c.100\,mV/s}$ (a), $PPy_{6c.100\,mV/s}Pd_{t=10\,min}$ (b), $PPy_{6c.100\,mV/s}Pd_{t=5\,min}$ (c) and $PPy_{6c.100\,mV/s}Pd_{t=overnight}$ (d); (C) $PPy_{60\,s}$ (a), $PPy_{60\,s}Pd_{t=10\,min}$ (b) and $PPy_{60\,s}Pd_{t=5\,min}$ (c); (D) $PPy_{120\,s}$ (a), $PPy_{120\,s}Pd_{t=10\,min}$ (b), $PPy_{120\,s}Pd_{t=5\,min}$ (c) and $PPy_{120\,s}Pd_{t=overnight}$ (d), in presence of 6 mM hydrazine in 0.5 M KCl (pH = 6), at υ = 50 mV/s.

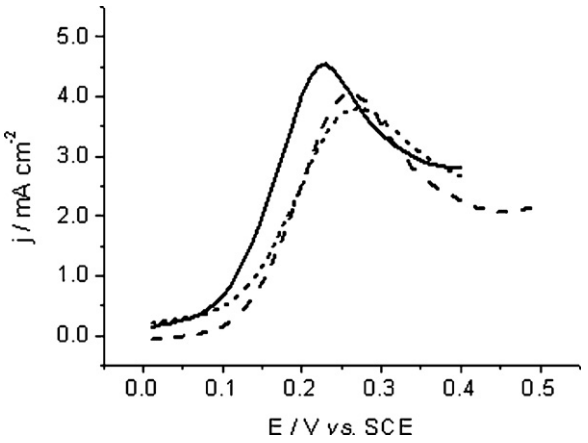

Fig. 10. Linear sweep voltammograms of the modified electrode $PPy_{120\,s}Pd_{10\,min}$ (short broken line), $PPy_{6c\_100\,mV/s}Pd_{5\,min}$ (full line), and $PPy_{6c\_100\,mV/s}$ $Pd_{overnight}$ (broken line), in presence of 6 mM hydrazine in 0.5 M KCl (pH = 6); υ = 50 mV/s.

Fig. 10 contrasts the behaviour of Pd (overnight electroless deposition on $PPy_{6c\_100\,mV/s}$) to that of $PPy_{6c\_100\,mV/s}Pd_{5\,min}$ and $PPy_{120\,s}Pd_{10\,min}$ electrodes, which display the best electrocatalytic activity towards the oxidation of HZ. Recalling the images presented in Fig. 7B and D, the importance of attaining a high surface density of small Pd particles for observing the aimed electrocatalytic properties is evident.

4. Conclusions

PPy films displaying similar electroactivities can be prepared using rather different electrochemical conditions, i.e., the oxidative conversion of PPy layers deposited potentiodynamically with 4 and 6 cycles at 50 and 100 mV/s respectively, and at 0.65 V constant potential for 120 s involves pretty close charges, about 6 mC cm^{-2}, and exhibits identical current peak shape and potential. However, just the polymer electroactivity cannot be used as comparative parameter when further modification of the PPy is envisaged, namely the incorporation of metal particles. As demonstrated in this work, strictly determined by the electrosynthesis conditions are the film morphology, porosity and surface area (PPy synthesised by potential cycling is formed by larger nodules than the potentiostatically deposited one) characteristics with particular relevance for the electroless precipitation of Pd on PPy.

EQCM data provided evidence on the role of the polymer surface features for the electroless precipitation of Pd: the initial rate of the Pd uptake is higher for films with regular morphology ($PPy_{120\,s}$) than when PPy with rough surfaces ($PPy_{6c\_100\,mV/s}$) are used, in spite of the similar final increase in mass observed for 10 min. Since two events must be considered, the incorporation palladium ionic species as PPy dopants and the electroless precipitation of Pd(0) at the active sites of the PPy surface, it is reasonable to assume that the rate and extent of both processes depend on the PPy surface nature. However, for electrocatalytic purposes, the relevant factor is the Pd(0) incorporation.

As assessed by XPS analysis of the samples (after Pd uptake for 5 and 10 min), the Pd^0/Pd_{ox} ratios are of about the same order of magnitude for both modified PPy films; the Pd/N ratios, are considerably larger for $PPy_{120\,s}$ than for $PPy_{6c\_100\,mV/s}$, loaded with Pd either for 5 or 10 min, but decline with the increase in time of the electroless precipitation process. In agreement with previous studies, these results indicate that after 5 min deposition the Pd particles are well spread over the entire PPy surface whereas Pd particles aggregation shall occur for longer periods. SEM and AFM images of the PPy–Pd films provided good support to this interpretation.

The PPy–Pd modified electrodes reveal significant catalytic anodic currents towards the oxidation of hydrazine in KCl solution. The best behaviour is found for $PPy_{6c\_100\,mV/s}Pd_{5\,min}$ film, with which a considerable increase in the rate and a decrease in the overpotential required for HZ oxidation is achieved, in comparison to Pd coated PPy electrodes. The beneficial catalytic effect of the small sized incorporated Pd particles is also seen in the modified $PPy_{120\,s}$ films loaded with Pd for 5 and 10 min, where a slight lower current is generated but a shift in the potential to less positive values is observed. As a result of Pd particles aggregation, $PPy_{6c\_100\,mV/s}Pd_{10\,min}$ modified electrodes present a relatively poorer response. The collected information show that PPy–Pd modified electrode with interesting electrocatalytic properties can be prepared by the methodology employed in this work. However care must be taken both in choosing the electropolymerization conditions and in avoiding a disadvantageous increase on the amount and size of the incorporated Pd particles.

Acknowledgments

The authors acknowledge Dr. Ana Viana for the AFM images. L.M. Abrantes thanks the EU for the financial support to attend the "COST Chemistry D36 3rd Workshop and 5th Management Committee Meeting", where this work has been presented. A. Mourato (SFRH/BPD/35036/2007) and J.F. Cabrita (SFRH/BD/47703/2008) gratefully acknowledge the "Fundação para a Ciência e Tecnologia" for financial support.

References

[1] M. Trueba, S.P. Trasatti, S. Trasatti, Mater. Chem. Phys. 98 (2006) 165–171.
[2] Z.A. Hu, L.J. Ren, X.J. Feng, Y.P. Wang, Y.Y. Yang, J. Shi, L.P. Mo, Z.Q. Lei, Electrochem. Commun. 9 (2007) 97–102.
[3] S.W. Huang, K.G. Neoh, C.W. Shih, D.S. Lim, E.T. Kang, H.S. Han, K.L. Tan, Synth. Met. 96 (1998) 117–122.
[4] M. Ilieva, V. Tsakova, W. Erfurth, Electrochim. Acta 52 (2006) 816–824.
[5] M. Ocypa, M. Ptasinska, A. Michalska, K. Maksymiuk, E.A.H. Hall, J. Electroanal. Chem. 596 (2006) 157–168.
[6] A.P. O'Mullane, S.E. Dale, T.M. Day, N.R. Wilson, J.V. Macpherson, P.R. Unwin, J. Solid State Electrochem. 10 (2006) 792–807.
[7] A. Mourato, Synthesis and characterisation of electroactive polymer–metal nanoparticle catalyst composites, PhD Thesis, Universidade de Lisboa, 2007.
[8] A. Mourato, A.S. Viana, J.P. Correia, H. Siegenthaler, L.M. Abrantes, Electrochim. Acta 49 (2004) 2249–2257.
[9] A. Drelinkiewicz, M. Hasik, M. Kloc, Catal. Lett. 64 (2000) 41–47.
[10] Z.H. Ma, K.L. Tan, E.T. Kang, Synth. Met. 114 (2000) 17–25.
[11] E.T. Kang, Y.P. Ting, K.G. Neoh, K.L. Tan, Synth. Met. 69 (1995) 477–478.
[12] M. Hasik, A. Bernasik, A. Drelinkiewicz, K. Kowalski, E. Wenda, J. Camra, Surf. Sci. 507–510 (2002) 916–921.
[13] V.W.L. Lim, E.T. Kang, K.G. Neoh, Synth. Met. 123 (2001) 107–115.
[14] M. Hasik, A. Bernasik, A. Adamczyck, G. Malata, K. Kowalski, J. Camra, Eur. Polym. J. 39 (2003) 1669–1678.
[15] V. Selvaraj, M. Alagar, I. Hamerton, J. Power Sources 160 (2006) 940–948.
[16] I. Becerik, F. Kadirgan, J. Electroanal. Chem. 436 (1997) 189–193.
[17] M.A. DelValle, F.R. Diaz, M.E. Bodini, T. Pizarro, R. Cordova, H. Gomez, R. Schrebler, J. Appl. Electrochem. 28 (1998) 943–946.
[18] I. Dodouche, F. Epron, Appl. Catal. B: Environ. 76 (2007) 291–299.
[19] G. Chen, Z. Wang, T. Yang, D. Huang, Di. Xia, J. Phys. Chem. B 110 (2006) 4863–4868.
[20] C.R.K. Rao, D.C. Trivedi, Catal. Commun. 7 (2006) 662–668.
[21] M.R. Vilar, S. Boufi, A.M. Ferraria, A.M. Botelho do Rego, J. Phys. Chem. C 111 (2007) 12792.
[22] D.A. Buttry, M.D. Ward, Chem. Rev. 92 (1992) 1355–1379.
[23] S.J. Choi, S.-M. Park, J. Electrochem. Soc. 149 (2002) E26.
[24] J.N. Barisci, R. Stella, G.M. Spinks, G.G. Wallace, Electrochim. Acta 46 (2000) 519–531.
[25] M. Skompska, M.A. Vorotyntsev, J. Solid State Eletrochem. 8 (2004) 360–368.
[26] E. Tamburri, S. Orlanducci, F. Toschi, M.L. Terranova, D. Passeri, Synth. Met. 159 (2009) 406–414.
[27] L.M. Abrantes, J.P. Correia, Mater. Sci. Forum 191 (1995) 235–240.
[28] E.T. Kang, K.G. Neoh, K.L. Tan, Surf. Interface Anal. 19 (2004) 33–37.
[29] C.D. Wagner, A.V. Naumkin, A. Kraut-Vass, J.W. Allison, C.J. Powell, J.R. Rumble Jr., NIST X-ray Photoelectron Spectroscopy Database, Standard Reference Database 20, Version 3.5, National Institute of Standards and Technology (NIST).
[30] J.L. Yague, N. Agullo, S. Borrós, Chem. Vapor Dep. 15 (2009) 128–132.
[31] G. Beamson, D. Briggs, High Resolution XPS of Organic Polymers. The Scienta ESCA300 Database, John Wiley & Sons, New York, 1992.

[32] P. Neves, M. Arronte, R. Vilar, A.M. Botelho do Rego, Appl. Phys. A 74 (2002) 191–199.
[33] D. Briggs, M.P. Seah (Eds.), Practical Surface Analysis, 2nd ed., Wiley, New York, 1996.
[34] S.M. Golabi, H.R. Zare, J. Electroanal. Chem. 465 (1999) 168–176.
[35] J Li, X. Lin, Sens. Actuators B 126 (2007) 527–535.
[36] M.R. Majidi, A. Jouyban, K. Asadpour-Zeynali, Electrochim. Acta 52 (2007) 6248–6253.
[37] N. Malekia, A. Safavi, E. Farjamia, F. Tajabadi, Anal. Chim. Acta 611 (2008) 151–155.
[38] C. Batchelor-McAuley, C.E. Banks, A.O. Simm, T.G.J. Jones, R.G. Compton, Analyst 131 (2006) 106–110.